Investigation of the Factors Affecting the Cogging Torque of a Permanent Magnet Brushed DC Motor

Aula Ghazi Salim [*], Amer Mejbel Ali [**]

[*] Electrical Engineering Department, College of Engineering, Mustansiriyah University, Baghdad, Iraq
Email: aula.Salim@uomustansiriyah.edu.iq
https://orcid.org/ 0009-0000-8388-8014

[**] Electrical Engineering Department, College of Engineering, Mustansiriyah University, Baghdad, Iraq
Email: dramerma@uomustansiriyah.edu.iq
https://orcid.org/0000-0002-9984-3109

Abstract

Cogging torque disadvantages permanent magnet DC motors (PMDC), creating vibration and audible noises. This research investigates the factors affecting the cogging torque of a permanent magnet-brushed DC motor used to operate automobile windshield wipers by implementing some design changes by using the finite element analysis (FEA) based on Maxwell 2D software. These factors include changing the air gap length, slot opening, embrace factor, magnet edge inset (pole arc offset), skewing angle, and magnet type to study the amount of reduction and increase in cogging torque and its effect on the motor's efficiency. We conclude from the results of the FEM simulation that when changing the parameters of the factors, we will notice a clear effect on cogging torque and motor efficiency.

Keywords- Cogging torque, Permanent magnet brushed DC motor, Finite element analysis, Maxwell 2D.

I. INTRODUCTION

Brushed DC motors are widely used in various applications, including toys, automobile gear motors, and power equipment. Since they can run at high speeds (up to 20,000 rpm) straight from a battery, DC motors have one major advantage over AC motors. They come in various sizes and forms, are inexpensive, and are simple to drive [1]. The DC motor dominated the electric machinery used in all variable-speed motor driving applications until the advent of dependable, high-power solid-state switching devices. In the automotive industry, DC motors were the most cost-effective option for blowers, power windows, windshield wipers, and cranking motors [2]. Permanent magnet machines are increasingly used in industrial applications. As their cost continues to drop, they present a low-size, high-power-density, and highly efficient alternative to traditional machines that have the potential to dominate the industrial applications market. An inherent torque ripple in PM machines' design is one of their main disadvantages. This parasitic ripple can cause drive system issues, acoustic noise, and mechanical vibration. A major factor in torque ripple in PM machines is cogging torque, which is brought on by unequal air-gap permeance between PMs and stator slots. In the process of designing a PM machine, minimizing this ripple is crucial [3]. The benefits of using PMs in the construction of electrical machines are that the field excitation system absorbs no electrical energy, so there are no excitation losses, which results in a significant increase in efficiency, Greater output power and torque per volume compared to electromagnetic excitation, higher dynamic performance compared to motors that are excited by electromagnetic, Simplifying the process of building and maintaining, Price reductions for specific equipment types. When there is no excitation winding and no power loss, a PM can create a magnetic field in an air gap. The energy of the magnetic field is not maintained by external energy; it is merely altered by it. A PM is characterized by its B-H hysteresis loop, much like any other ferromagnetic material. PMs are ferromagnetic materials with a broad hysteresis loop, often known as hard magnetic materials. Currently, electric motors use three classes of PMs: Alnicos (Al, Ni, CO, Fe), Ceramics (ferrites), and Rare-earth materials, i.e., samarium-cobalt (SmCo) and neodymium ferrite boron (NdFeB) [4]. Utilizing finite element method (FEM) software to modify the design and increase the torque efficiency of a brushed permanent magnet DC motor in order to save material usage. It compares simulation results with actual measurements of the test motor to validate the accuracy of the model through three stages of modifications that are implemented to achieve the desired torque efficiency and higher overall motor efficiency [5]. One significant PMDC motor drawback that causes noise and shaft vibrations is cogging torque. To minimize cogging torque in PMDC motors by introducing structural design modifications and utilizing analytical models for optimal configuration selection and material

characteristics. The analysis involves the use of Finite Element Analysis (FEA) to evaluate the performance of existing machine designs, with a specific focus on cogging torque and average torque as performance metrics for determining the best permanent magnet material and pole width combinations [6].

This paper aims to study the factors affecting the cogging torque and efficiency of a 50W, 12V PMDC motor used to operate the automobile windshield wiper using finite element analysis (FEA) based on Maxwell 2D software. These factors include changing the air gap length, slot opening, embrace factor, magnet edge inset (pole arc offset), skewing angle, and magnet type by modifying the motor design.

II. MATHEMATICAL BACKGROUND

In a PMDC motor, cogging torque is produced through the interaction of the rotor slots and the permanent magnets in the stator. Because the slots make the cogging torque, the reluctance in the air gap varies as the rotor rotates. The reluctance changes when the magnetic flux moves from the rotor to the stator. Initially passing through the rotor and magnets, the magnetic flux then moves on to the air gap and stator before returning in a similar way. Equation (1) is a simplified equation for calculating the cogging torque [5].

$$T_c = -\frac{1}{2}\varphi_\delta^2 \frac{dR}{d\theta} \quad (1)$$

Where φ_δ is the magnetic flux crossing the air gap, R is the reluctance through the flux passes, θ is the mechanical rotor position, and dθ is the change in position of the rotor [2].

The amount of energy stored in the air gap and the cogging torque as a force can be calculated using virtual labor. According to this definition, the cogging torque is given by Equation (2) [5].

$$T_c = -\frac{dW}{d\theta} \quad (2)$$

Where W represents the stored energy, changing the position of the rotor affects the stored energy and magnetic flux. Rewriting the cogging torque in terms of flux Φm and coercive force F_c yields in Equation (3)

$$T_c = \frac{1}{2} F_c \frac{d\text{Φ}m}{d\theta} \quad (3)$$

The Equation (4) for calculating the efficiency(η) of PMDC motor is given [7]:

$$\eta = \frac{P_{out}}{P_{in}} * 100\% \quad (4)$$

To determine the electrical power input to a PMDC motor, Equation (5) must equal the sum of the motor's total loss (P_l) and mechanical power output (P_{out}) [7]:

$$P_{in} = P_{out} + P_l \quad (5)$$

$$P_{out} = T_l\, \omega \quad (6)$$

$$P_l = P_{mech} + P_{cu} + P_{core} + P_B + P_{stray} \quad (7)$$

Equation (8) represents the calculation of mechanical losses (P_{mech})

$$P_{mech} = T_f \omega \quad (8)$$

Where T_f is friction torque (N.m) and ω is Angular velocity (rad/sec).

Equation (9) represents the calculation of armature copper losses (P_{cu}) is

$$P_{cu} = RI^2 \quad (9)$$

Where R is motor windings resistance (Ohm) and I is Input current (A) [8].

Core losses P_{core} are due to the sum of hysterical losses and eddy current losses as shown in Equation (10) [9,10,11]

$$P_{core} = P_{hyst} + P_{eddy} \quad (10)$$

$$P_{hyst} = K_h f B^{1.6} \quad (11)$$

$$P_{eddy} = K_e f^2 B^2 \quad (12)$$

Where:
P_{hyst}: hysteresis loss ($\frac{W}{m^3}$)
K_h: hysteresis loss coefficient
P_{eddy}: eddy current loss ($\frac{W}{m^3}$)
K_e: eddy current loss coefficient
B: flux density amplitude within the material
f: The applied excitation frequency equals the PMDC motors' electrical frequency. Calculate it by [12]:

$$f = pn * \frac{2\pi}{60} \quad (13)$$

Where $p =$ the number of pole pairs.
Brush drop loss refers to the loss of motor brush power across contact potential, as in Equation (14).

$$P_B = V_{BD} I_a \quad (14)$$

Where V_{BD} = brush voltage drop (V), and I_a = armature current (A).
The computation of brush losses is based on the fact that the voltage drop across a set of brushes is generally consistent across a wide range of armature currents. Unless specifically mentioned otherwise, it is common to estimate the voltage decrease of the brush at 2 V [9, 13].
The stray losses (P_{stray}) are taken to be 1% of the input power (p_{in}) [9], given by:

$$P_{stray} = 0.01 P_{in} \quad (15)$$

III. MODELLING AND SIMULATION OF THE TESTED PMDC MOTOR

This article uses a 50W, 12V commercial permanent magnet brushed DC test motor to operate automotive windshield wipers. Figure (1a) illustrates the windshield wiper motor. This motor's cross-section is shown in Figure (1b). Firstly, reverse engineering was used to gain design information on this motor by disassembling it and measuring the measurements of each component in the motor, as shown in Table 1. Figure (1c) depicts the overall assembly of the test motor. Secondly, the windshield wipers were operated by a permanent magnet-brushed DC motor test model, as depicted in Figure (2). Measuring the motor's speed and current in any situation when the load changes is the aim; this data is regarded as program input, as shown in Table (2). Finally, Ansys Maxwell finite element analysis (FEM) based on Maxwell 2D software and RMxprt are used to model, simulate, and analyze motor performance.
RMxprt is an Ansys-Maxwell Suite template-based design tool used to develop a customized machine design flow in order to satisfy the requirements for increased efficiency. RMxprt can assess machine performance and decide on initial scaling [14]. Maxwell 2D may be completely configured automatically by RMxprt for transient electromagnetic FEM analysis. The design sheets in RMxprt consist of a list of all required inputs, computed parameters, and a graphical depiction of the waveforms [15]. Figure (3) represents the model of the PMDC motor by RMxprt according to the dimensions, specifications, and materials, as shown in Figure (4).

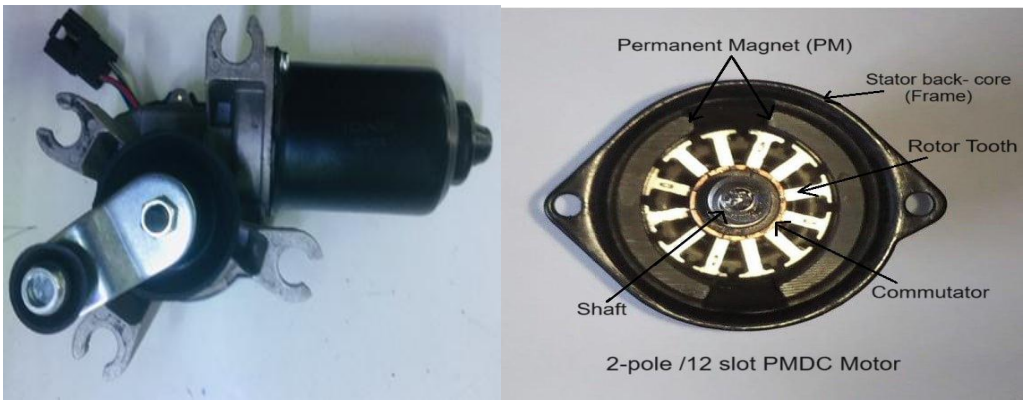

(a) (b)

ISSN: 2710-2165

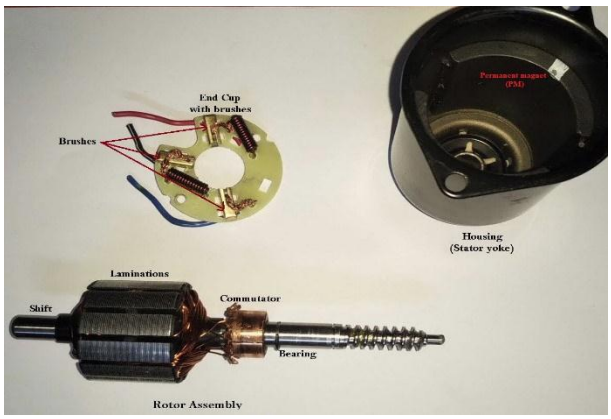

(c)

Figure 1. Permanent Magnet-Brushed DC test motor

Table 1 Specifications of Reference PMDC Motor

Parameter	Value	Unit
Rated speed	1944	rpm
Stator Outer Diameter	56.6	mm
Stator Inner Diameter	41	mm
Stator Length	73.2	mm
Stator Stack factor	1	__
Offset	0	mm
Embrace factor	0.786	__
Magnet Length	48.8	mm
Magnet Thickness	5.73	mm
Stator Types of steel	Steel_1008	__
Magnet Type of the Stator	Ceramic (ferrite) [9]	__
Rotor Diameter (inner)	10	mm
Rotor Length	30	mm
Number of Slots	12	__
Conductors per Slot	42	__
Coil Pitch	5	__
Wire Wrap	0.05	mm
Wire Diameter	0.5	mm
Skew Width	0	deg
Rotor Types of steel	M600-50A	__
Slot opening height (Hs0)	1.2	mm
Slot wedge height (Hs1)	1	mm
Slot body height (Hs2)	8	mm
Slot opening width (Bs0)	2.5	mm
Slot wedge maximum width (Bs1)	6.4	mm
Slot body bottom width (Bs2)	2.4	mm
Commutator Diameter	18.3	mm
Commutator Length	12.2	mm
Commutator Insulation	0.2	mm
Brush Width	3.7	mm
Brush Length	9.7	mm

ISSN: 2710-2165

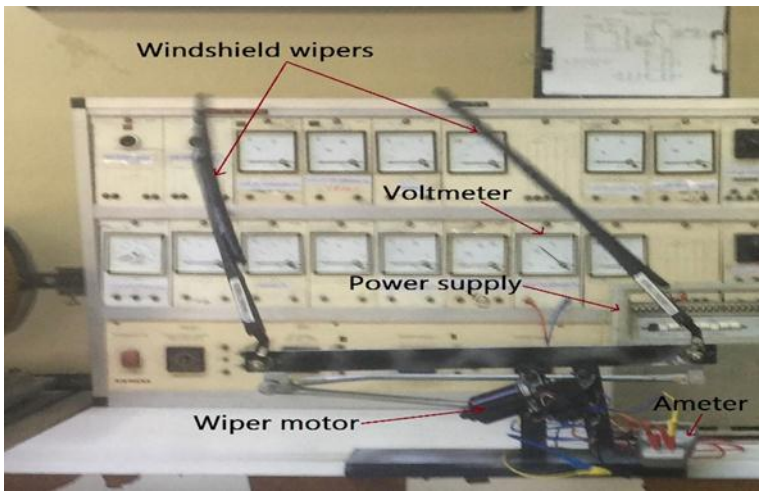

Figure 2. A Model for Operating the Windshield Wipers

Table 2 Test Results at High Speed

Parameter	Value	Unit
Current	6.42	A
Speed	1944	rpm
Torque	0.2456	N.m
Input power	77.04	W

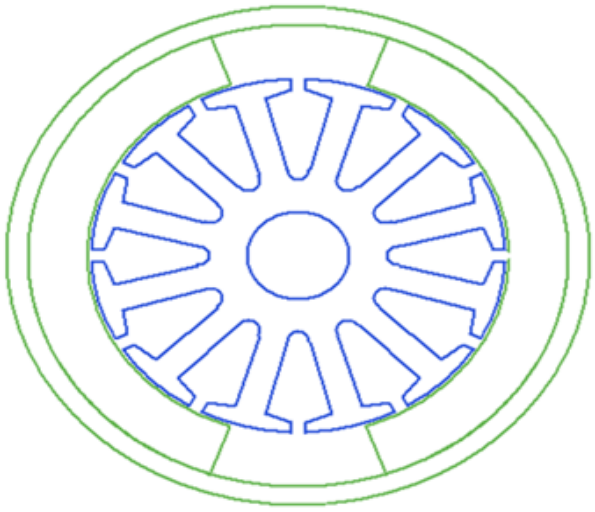

Figure 3. PMDC Motor Model by RMxprt

ISSN: 2710-2165

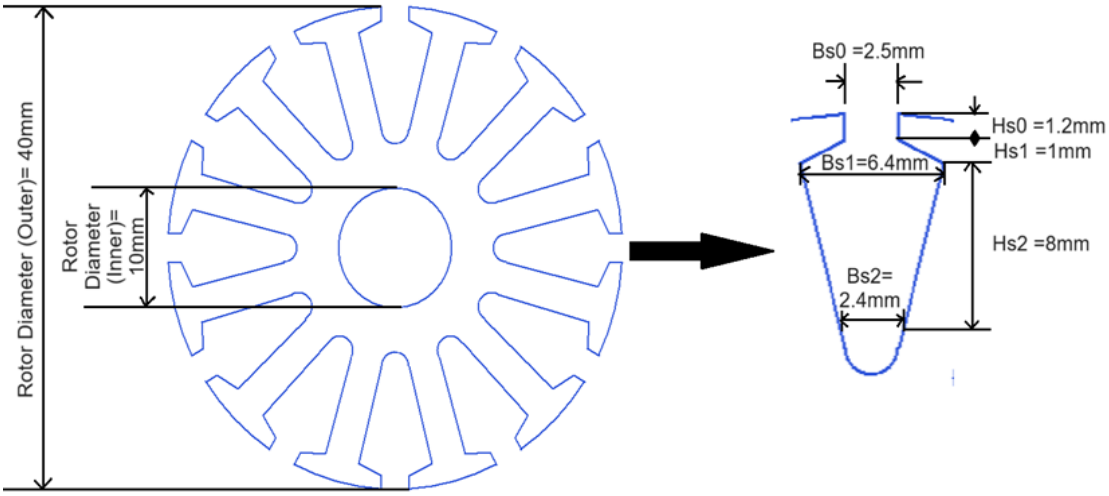

Figure 4. Rotor Lamination Model by RMxprt

Create a Maxwell 2D design from RMxprt. Maxwell2D is a finite element analysis (FEA) software designed to solve electromagnetic field issues in two dimensions. Maxwell2D enables engineers to model and simulate electromagnetic equipment and systems such as motors, generators, transformers, actuators, and more. Maxwell2D allows users to investigate a variety of electromagnetic phenomena such as magnetic flux, magnetic field intensity, electromagnetic forces, torque, losses, and others. Engineers can use it as a platform to maximize their electromagnetic devices' efficiency, dependability, and performance, guaranteeing that they satisfy the required specifications [14,15]. Figure (5) depicts the Maxwell 2D motor model, and Figure (6) shows the finite element meshing of the test motor.

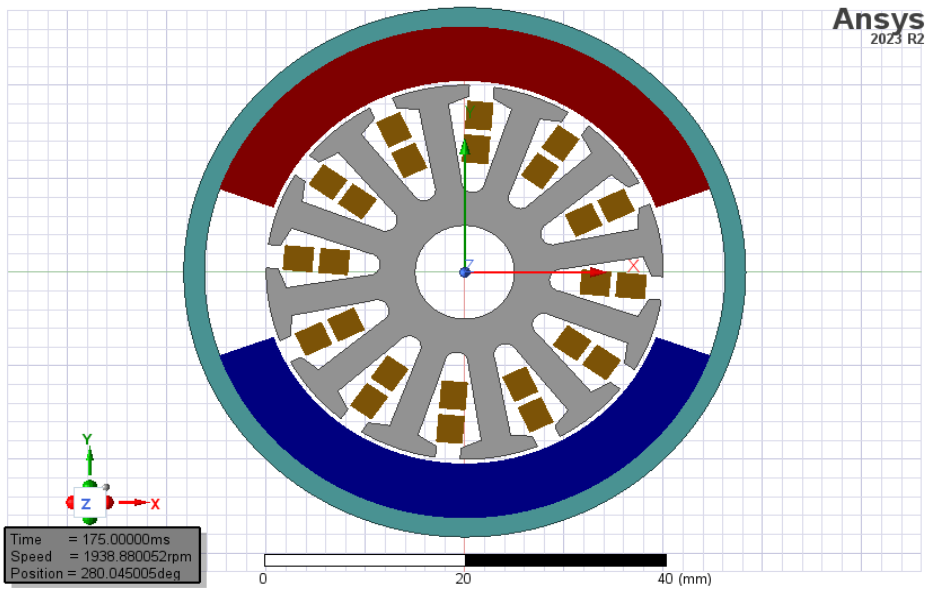

Figure 5. 2D Model Representation of the PMDC Motor by Maxwell 2D

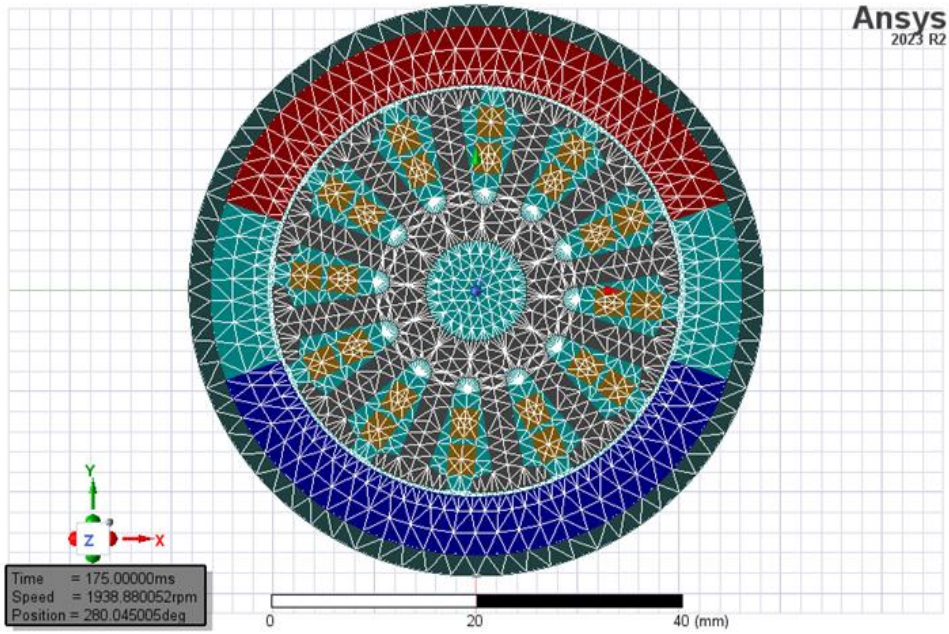

Figure 6. Finite Element Mesh of the PMDC Motor by Maxwell 2D

IV. RESULTS AND DISCUSSION

In this paper, we discuss the results of simulating the factors affecting on the cogging torque of a permanent magnet-brushed DC motor as follows:

1) Effect of Air-Gap Length on Cogging Torque

The FEA model with an air-gap length of a PMDC motor is shown sectionally in Figure (7). The air-gap length is changed by changing the outer diameter of the rotor values of (40.4, 40, 39.6, and 39) mm; in contrast, the air-gap lengths are (0.3, 0.5, 0.7, 1) mm, and the various cogging torque waveforms are obtained by conducting a finite element analysis as shown in Figure (8) and Table (3).

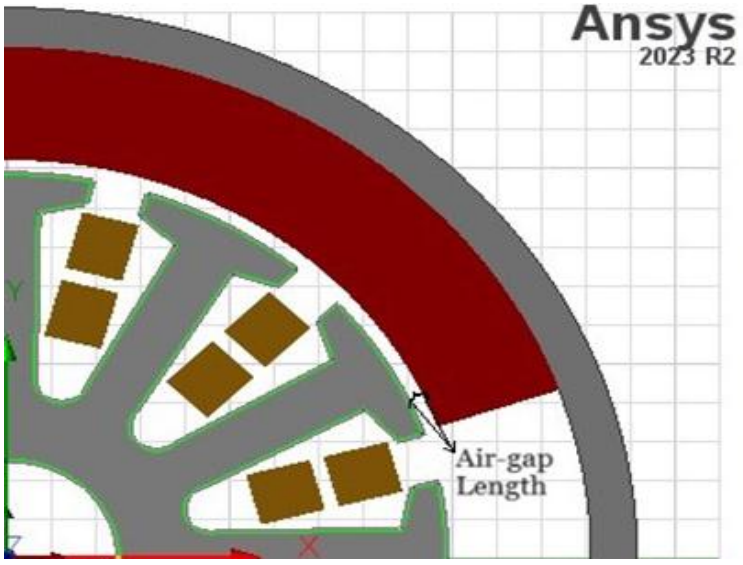

Figure 7. Sectional View of PMDC Model with Change in Air-Gab Length by Maxwell 2D

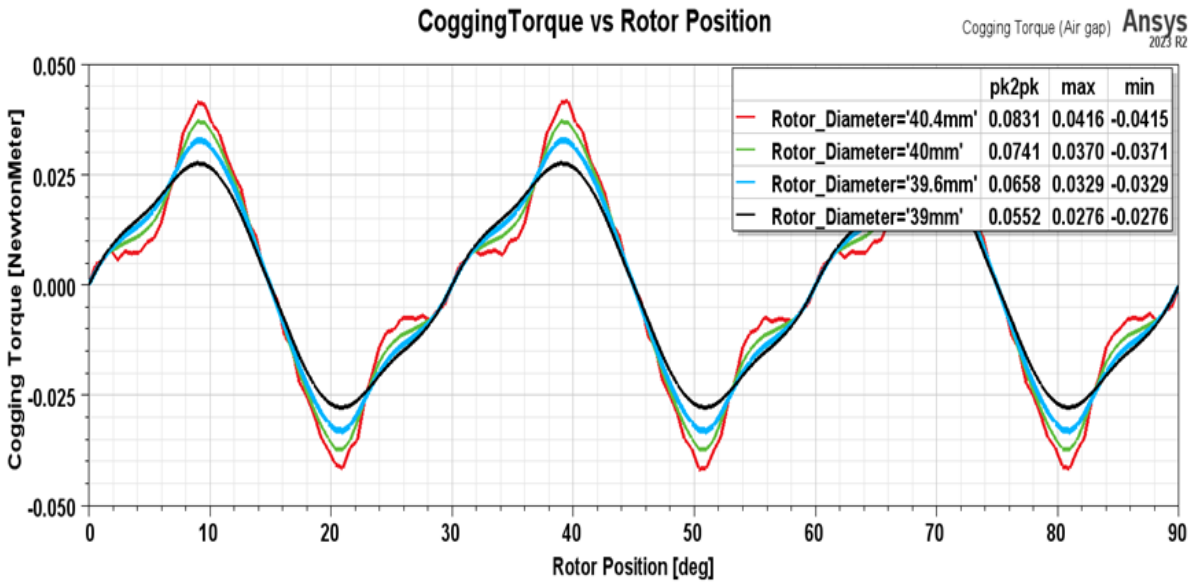

Figure 8. Effect of Changing Air-Gap Length on Motor Cogging Torque

Table 3 Effect of changing Air-Gap Length on Motor Cogging Torque and Efficiency

Rotor Diameter (mm)	Air-gap Length (mm)	Pk-Pk Cogging Torque (N.m)	Efficiency %
40.4	0.3	0.0831	64.72
40	0.5	0.0741	63.881
39.6	0.7	0.0658	62.36
39	1	0.0552	59.83

Figure (8) and Table (3) the simulated results show that when the air-gap length is 0.3mm (reducing the air-gap length from 0.5mm (default) to 0.3mm), the cogging torque from peak-to-peak increases from 0.0741N.m to 0.0831N.m with an increase in motor efficiency from 63.88% to 64.72%.When the air-gap length was increased from 0.5mm to 1mm, the cogging torque from peak-to-peak decreased from 0.0741N.m to 0.0552 N.m with a decrease in motor efficiency from 63.88% to 59.83%.

Increasing the air gap length reduces $\frac{dR}{d\theta}$ Equation (1) increases its reluctance, thereby reducing cogging torque. As a result, the φ_δ is lowered. In turn, cogging torque is reduced also [5].

2) Effect of Slot Opening on Cogging Torque

The permanent magnet-brushed DC motor rotor has slots for the armature windings. These slots can influence how magnetic flux is distributed in the motor. The cogging torque and the distribution of the magnetic field can be affected by the size, geometry, and, in especially, the opening width of the slots [16]. The FEA model of a PMDC motor with a slot opening is shown in the section in Figure (9). The slot opening width is changed from 1.5mm to 3.5mm (default is 2.5mm), and the different cogging torque waveforms are obtained through FEA analysis.

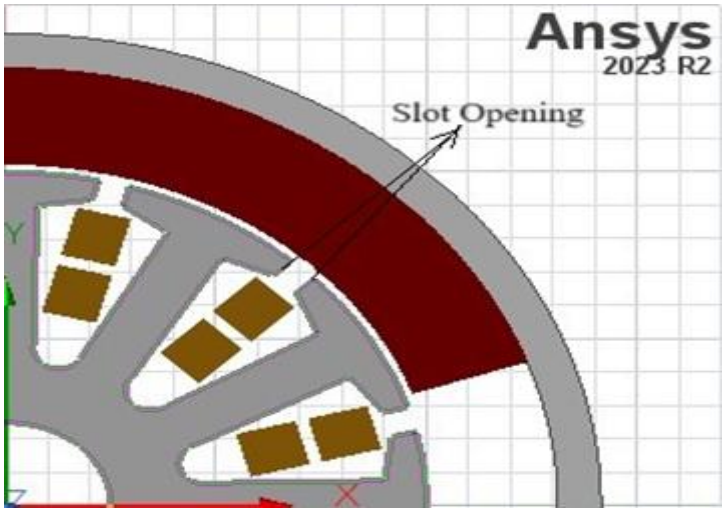

Figure 9 Sectional view of PMDC model with change in slot opening by Maxwell 2D

The reduction of the slot opening width from 2.5mm to 1.5mm, as shown in Figure (10) and Table (4), increases motor efficiency and peak-to-peak cogging torque. Specifically, we observe that the motor efficiency increases from 63,881% to 63,925%, and the cogging torque peak-to-peak value increases from 0,0923 N.m. to 0,0475 N.m. When the slot opening width is expanded from 2.5mm to 3.5mm, the cogging torque from peak-to-peak decreases from 0.0741N.m to 0.0475N.m with a decrease in motor efficiency from 63.881% to 62.835%.

Widening the slot opening reduces cogging torque, allowing for better alignment of the magnetic field lines and smoother transitions as the rotor rotates. As a result, optimizing the slot opening size requires balancing and minimizing cogging torque while preserving other desired motor properties such as efficiency, power density, and noise levels [17].

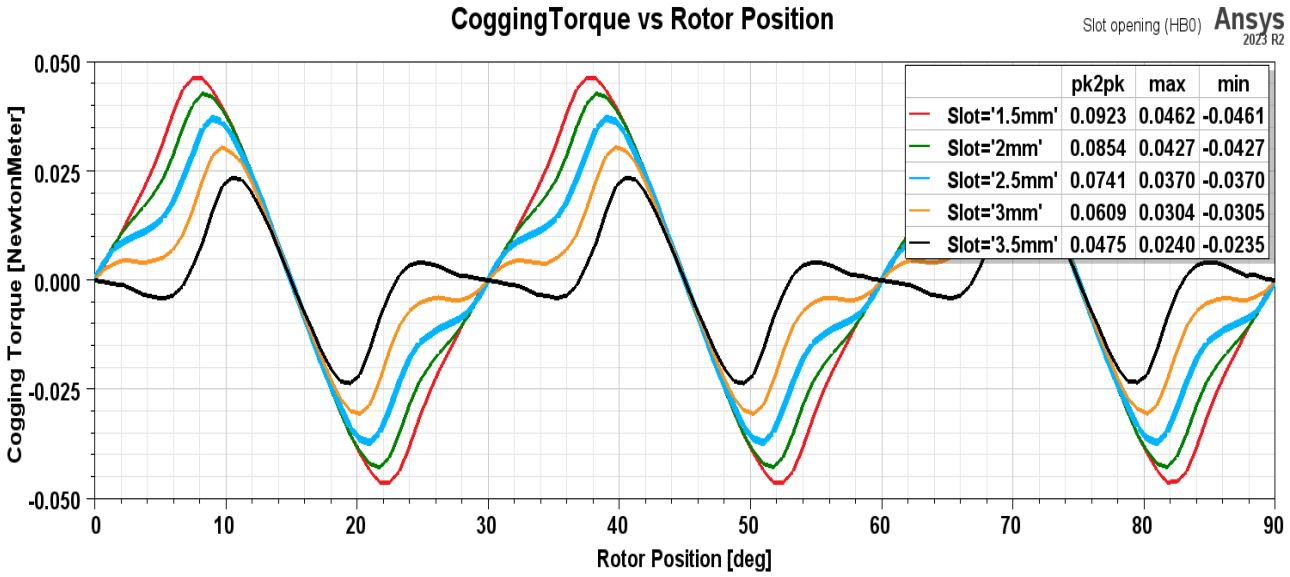

Figure 10. Effect of changing Slot Opening on Motor Cogging Torque

Table 4 Effect of changing Slot Opening on Motor Cogging Torque and Efficiency

Slot Opening (mm)	Pk-Pk Cogging Torque (N.m)	Efficiency %
1.5	0.0923	63.925
2	0.0854	63.891
2.5	0.0741	63.881
3	0.0609	62.856
3.5	0.0475	62.835

3) Effect of Skewing Angle on Cogging Torque

In permanent magnet-brushed DC motors, skewing of rotor slots is used to reduce cogging torque. A smoother magnetic field transition between the poles and teeth results from this skewing, which lessens the variation in magnetic forces that generate cogging torque. Skewing distributes cogging torque peaks over a larger mechanical angle. A smoother rotation results from this distribution's reduction of the cogging torque peaks' amplitude [18,19]. The FEA model's cross section for a PMDC motor with varying skew angle by Maxwell 3D is displayed in Figure (11). Note: Maxwell 3D was created by RMxprt, just as Maxwell 2D was created.

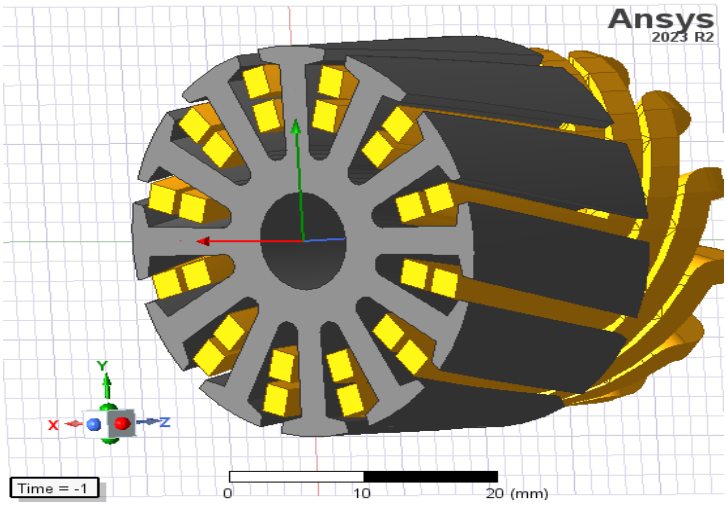

Figure 11. Cross section of PMDC model for skew angle by Maxwell 3D

Figure (12) and Table (5) show the change of skew angle from 0 deg (default) to 15 deg without changing the other parameters. The cogging torque waveform will change, and the peak-to-peak value of cogging torque will be reduced from 0.0359 N.m to 0.0231 N.m by (35.65% of the initial design) with a decrease in motor efficiency from 63.881% to 63.264%.

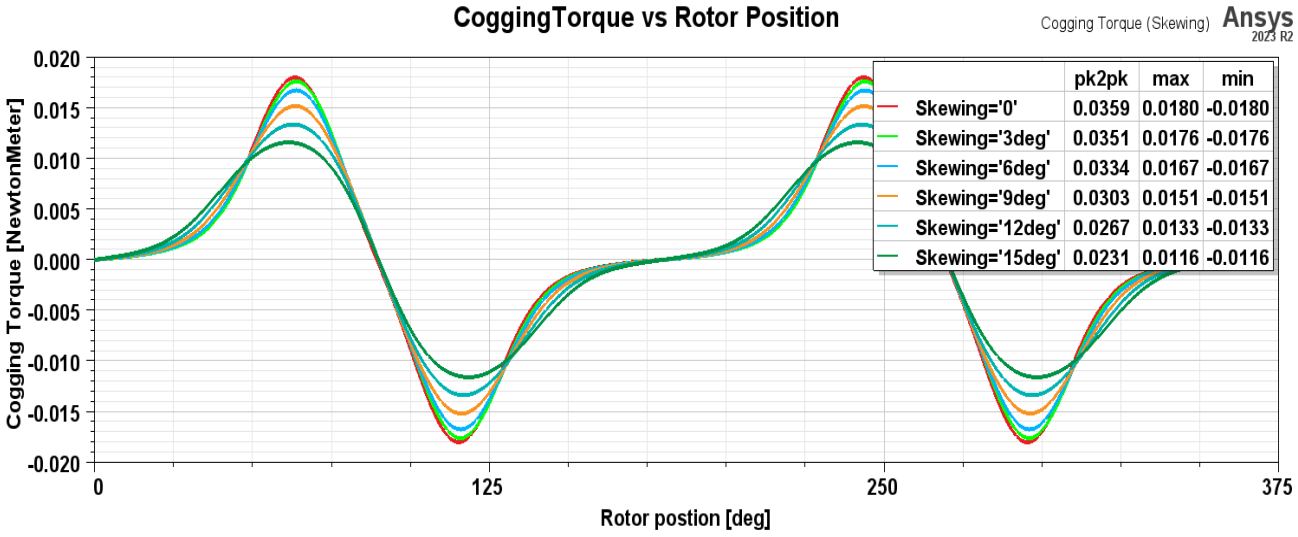

Figure 12. Effect of changing skew angle on Motor Cogging Torque

Table 5 Effect of changing skew angle on Motor Cogging Torque and Efficiency

Skew Angle (deg)	Pk-Pk Cogging Torque (N.m)	Efficiency %
0	0.0359	63.881
3	0.0351	63.731
6	0.0334	63.702
9	0.0303	63.654
12	0.0267	63.422

15	0.0231	63.264

4) Effect of Magnet Edge Inset (Pole Arc Offset) on Cogging Torque

The quarter sectional view of the FEA model for a PMDC motor with the stator poles' magnet edge inset (pole arc offset) is displayed in Figure (13).

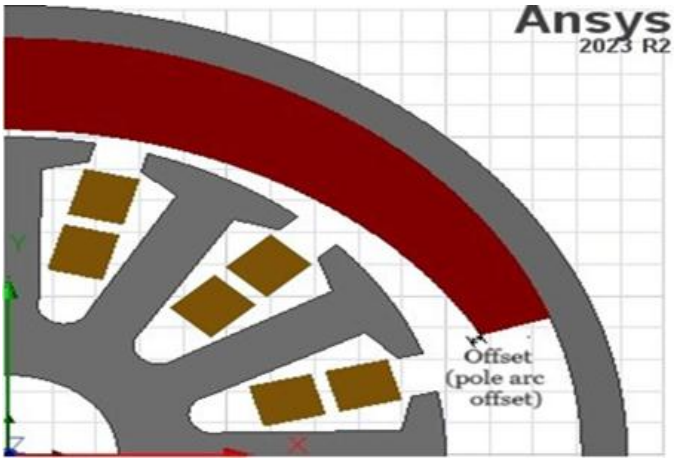

Figure 13. Cross sectional of PMDC model with change in pole arc offset in stator poles by Maxwell 2D

The pole arc offset is adjusted up to 3.0 mm without affecting other parameters. Finite element analysis produces a different cogging torque waveform. Peak-to-peak cogging torque can be decreased by altering the magnet edge inset, as shown in Figure (14). The lowest amount is reached when the magnet edge is 3mm inset while keeping the motor torque and back emf constant. The cogging torque peak-to-peak value is decreased from 0.0755 N.m. to 0.0177 N.m., a 76.56% decrease from the original model, with motor efficiency decreasing from 63.881% to 62.14%, as shown in Figure (14) and Table (6). Suppose the magnet edge inset is increased further. In that case, the air-gap flux density will gradually drop, resulting in lesser cogging torque and lower efficiency production during motor operation, so the cogging torque reduction must be balanced for smooth operation and high efficiency.

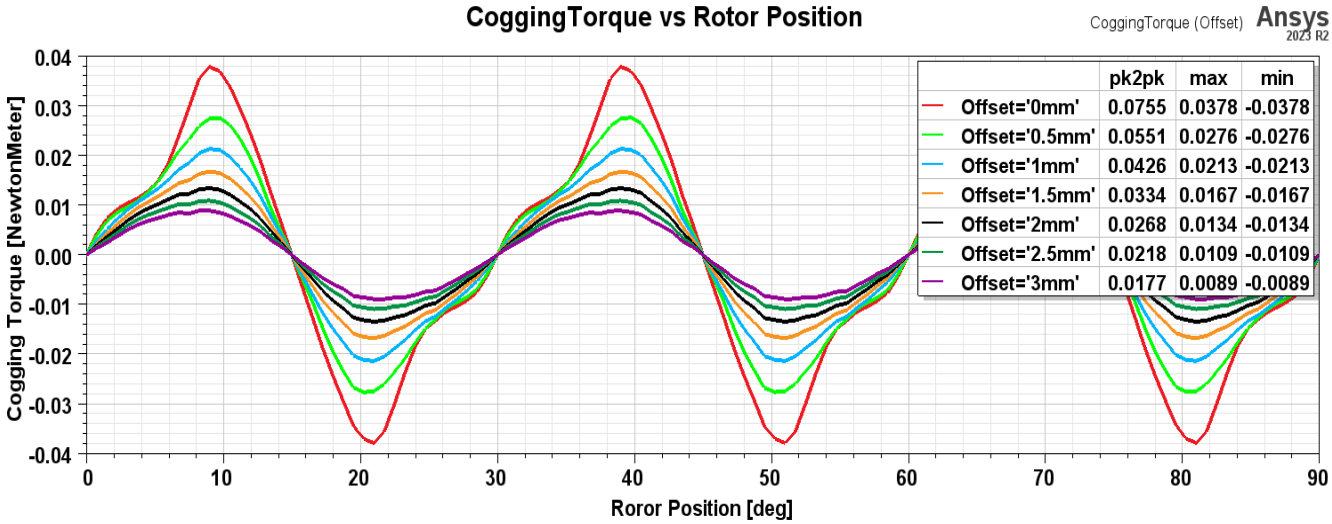

Figure 14. Effect of changing Pole Arc Offset on Motor Cogging Torque

Table 6 Effect of changing Pole Arc Offset on Motor Cogging Torque and Efficiency

Pole Arc Offset (mm)	Pk-Pk Cogging Torque (N.m)	Efficiency %
0	0.0755	63.881
0.5	0.0551	63.553
1	0.0426	63.315
1.5	0.0334	63.04
2	0.0268	62.754
2.5	0.0218	62.454
3	0.0177	62.14

5) Effect Embrace Factor on Cogging Torque

The embrace factor, also called the pole embrace factor, is a crucial design feature for permanent magnet-brushed DC motors, particularly in its effect on cogging torque [20]. The embrace factor is the magnetic pole arc divided by the pole pitch. Figure (15) displays half of the cross-sectional FEA model with a PMDC motor's embrace factor.

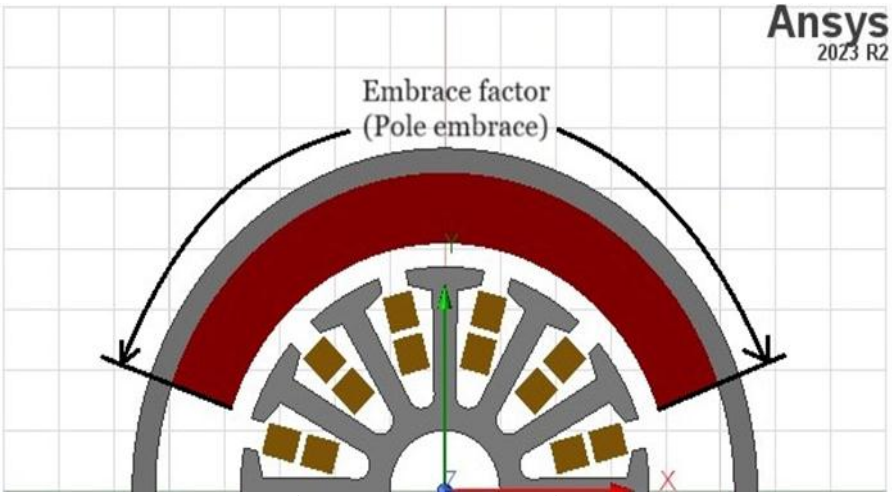

Figure 15. Cross sectional of PMDC model with embrace factor variation using Maxwell 2D

The default value of the embrace factor of the motor is 0.786. The embrace factor is changed from 0.7 to 0.8 without changing in other parameters. Figure (16) depicts various cogging torque waveforms resulting from a finite element analysis.

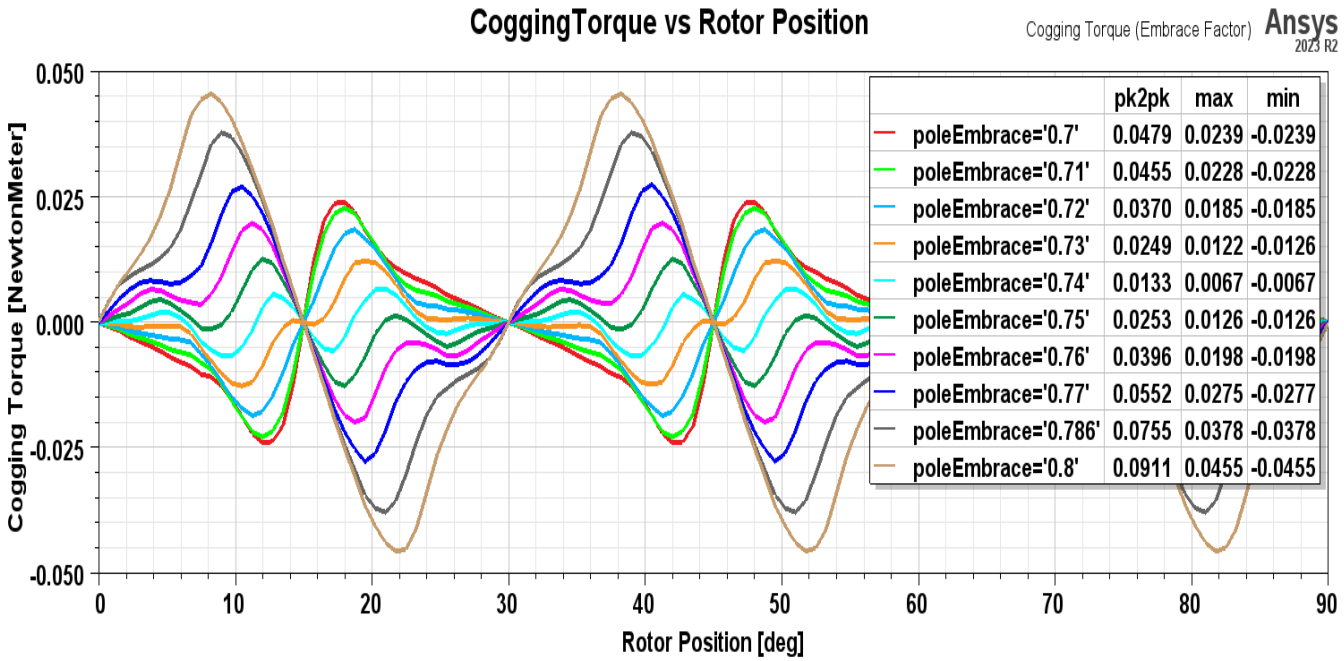

Figure 16. Effect of changing Embrace factor on Motor Cogging Torque

Table 7 Effect of changing Embrace factor on Motor Cogging Torque and Efficiency

Embrace Factor	Pk-Pk Cogging Torque (N.m)	Efficiency %
0.7	0.479	62.547
0.71	0.0455	62.761
0.72	0.037	62.988
0.73	0.0249	63.192
0.74	0.0133	63.394
0.75	0.0253	63.549
0.76	0.0396	63.71
0.77	0.0552	63.788
0.786	0.0755	63.881
0.8	0.0911	63.897

The above results show that when the embrace factor is changed from 0.7 to 0.74, the peak-to-peak cogging torque value is decreases from 0.0379 N.m. to 0.0133 N.m, and when the embrace factor is changed from 0.75 to 0.8, the peak-to-peak value of cogging torque increases from 0.0253 N.m to 0.0911 N.m. Therefore, modifying the embrace factor can improve the smooth and overall motor performance and the cogging torque reduction.

6) Effect of Changing Magnet Type on Cogging Torque

The influence of using different magnetic materials on cogging torque was investigated. The following are the magnet materials used in the analysis:

1) Alnico5
2) Ceramic (ferrite)
3) Neodymium Iron Boron (NdFeB)
4) Samarium Cobalt 24 (SmCo24)

The effect of these four different magnetic materials on cogging torque in terms of stator structure was studied by the effect of Magnetic Coercivity, as shown in Table (8).

Table.8 Magnetic Coercivity using different magnetic materials

Magnetic material	Magnetic Coercivity (A/m)
Neodymium Iron Boron (NdFeB)	-850000
Samarium Cobalt 24 (SmCo24)	-756000
Ceramic (ferrite)	-250000
Alnico5	-50970

Table (8) shows that the cogging torque decreases with less magnetic coercive force. As Figure (17) and Table (9) show, the cogging torque of NdFeB, SmCo24, ceramic (ferrite), and Alnico5 has peak-to-peak values of 0.255 Nm, 0.2027 Nm, 0.0397 Nm, and 0.0018 Nm, with reductions in motor efficiency values for all magnetic materials of 64.166%, 64.123%, 63.881%, and 29.705%.

Table.9 Cogging Torque Using Different Magnetic Materials

Magnetic Material	Cogging Torque (N.m)	Efficiency %
Neodymium Iron Boron (NdFeB)	0.255	64.166
Samarium Cobalt 24 (SmCo24)	0.2027	64.123
Ceramic (ferrite)	0.0397	63.881
Alnico5	0.0018	29.705

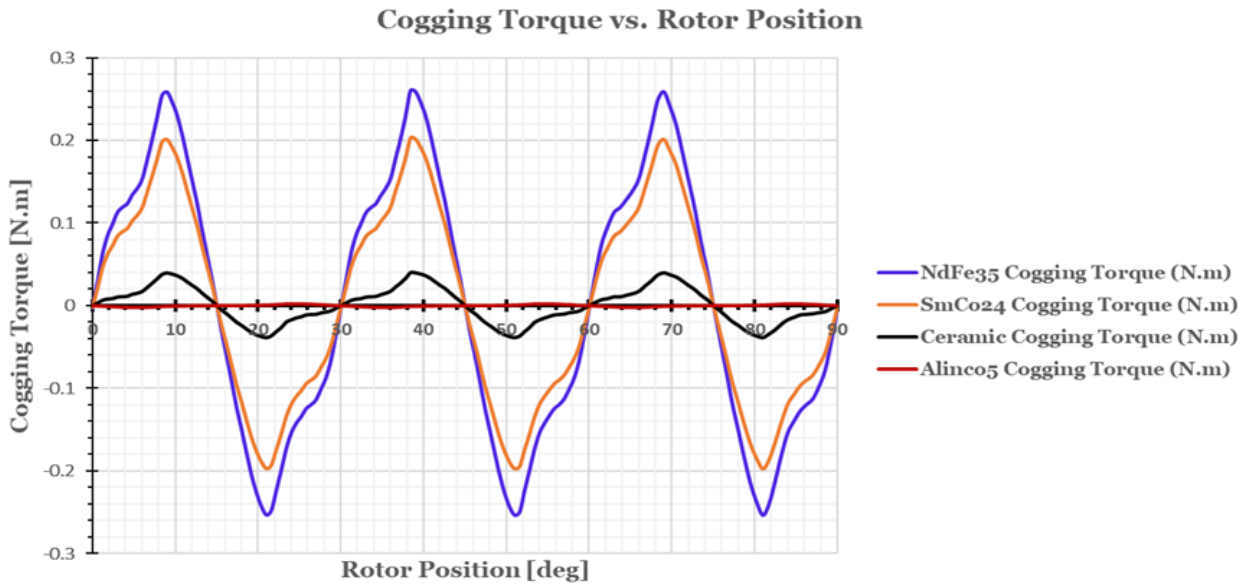

Figure 17. Effect of Magnet Type on Cogging Torque

V. CONCLUSION

In this research paper, the methods affecting on the cogging torque of the 50W, 12V, PMDC motor to operate car windshield wipers were investigated through FEM simulation using Maxwell 2D software. The effect of changing the air gap length, slot opening, skew angle, magnet edge inset (pole arc offset), embrace factor, and magnet type on reducing and increasing the cogging torque of the PMDC motor and its effect on the efficiency was studied. Reducing the air gap length and the slot opening width increases cogging torque and motor efficiency. When the air gap length is increased and the slot opening width is widened, the cogging torque decreases with a decrease in efficiency. Increase the skew angle and pole arc offset, decrease the cogging torque, and reduce the motor's efficiency. Also, the simulation results can be used to choose the best embrace factor to reduce the cogging torque. Based on design modifications and analysis, designers must select air gap length, suitable slot opening, and a magnetic edge inset (offset) with a suitable skew angle to balance between the low cogging torque to obtain smooth operation without vibrations and noise and between high efficiency.

ACKNOWLEDGMENT

The authors thank the Electrical Engineering Department, College of Engineering, Mustansiriyah University, Baghdad, Iraq.

REFERENCES

[1] J. Cros, G.C.R. Sincero, P. Viarouge. "Design Method for Brush Permanent Magnet Dc Motors". in 2009 IEEE International Electric Machines and Drives Conference. 2009. IEEE.
[2] A. Kiyoumarsi. "Analysis and Comparison of a Permanent-Magnet DC Motor with A Field-Winding DC Motor". Journal of Electrical Engineering and Technology, 2009. 4(3): p. 370-376.
[3] L. Dosiek, P. Pillay. "Cogging Torque Reduction in Permanent Magnet Machines". IEEE Transactions on industry applications, 2007. 43(6): p. 1565-1571.
[4] T. Gundogdu, G. Komurgoz. "Design of Permanent Magnet Machines with Different Rotor Type". International Journal of Electrical and Computer Engineering, 2010. 4(10): p. 1510-1515.
[5] Rasul Tarvirdilu-Asl., Reza. Z, and H.B. Ertan. "FEM-based design modifications and efficiency improvements of a brushed permanent magnet DC motor". in 2017 International Conference on Optimization of Electrical and Electronic Equipment (OPTIM) & 2017 Intl Aegean Conference on Electrical Machines and Power Electronics (ACEMP). 2017. IEEE.
[6] K. Harisudha, S.S. Afrose, K. Suresh. "Different Pole Arc Different Magnet Combination to Reduce the Cogging Torque in PMDC Motors". in 2017 IEEE International Conference on Power, Control, Signals and Instrumentation Engineering (ICPCSI). 2017. IEEE.
[7] Salah. I. S. TNATIN, Seliman A. M, and Fatma. R. M. A." Experimental and Simulation Study of a Permanent Magnet DC Motor at Steady State". 2017.

[8] S. B. Shah, B. Silwal, A. Lehikoinen. "Efficiency of an Electrical Machine in Electric Vehicle Application". Journal of the Institute of Engineering 2016;11(1), 20-29. doi:10.3126/jie. v11i1.14692.
[9] S.J. Chapman. Electric Machinery Fundamentals: McGraw-Hill Higher Education 2005; (pp. 533-632).
[10] Hussein. A.B, Amer. M.A." Losses Estimation of Switched Reluctance Motor". Paper presented at the 2023 Second International Conference on Advanced Computer Applications (ACA). doi: 10.1109/ACA57612.2023.10346958.
[11] Muhammed. A, Ali. B.Ö, Cengiz. İ. F. E, & Ahmet. M. V. Design and Modelling of Internal Permanent Magnet Motor. The International Journal of Energy and Engineering Sciences 2020; 5(2), 80-104.
[12] J.F. Gieras. Permanent Magnet Motor Technology: Design and Applications: CRC press. Taylor and Francis Group 2009; LLC.
[13] N. Boules. Design Optimization of Permanent Magnet DC Motors. IEEE Transactions on Industry Applications 1990; 26(4), 786-792.
[14] A. Kumar, R. Gandhi, R. Wilson, R. Roy. "Analysis of Permanent Magnet BLDC Motor Design with Different Slot Type". in 2020 IEEE International Conference on Power Electronics, Smart Grid and Renewable Energy (PESGRE2020). 2020. IEEE
[15] M.A. Hamdi, and F.A. Jumaa, "Improve the Efficiency of Brushless Permanent Magnet DC Motor By ANSYS–MAXWELL 3D/2D". Journal of Survey in Fisheries Sciences, 2023. 10(3S): p. 3031-3039.
[16] A.J. Kanapara, and K.P. Badgujar. "Performance Improvement of Permanent Magnet Brushless DC Motor Through Cogging Torque Reduction Techniques". in 2020 21st National Power Systems Conference (NPSC). 2020. IEEE.
[17] Ravisankar. B, Senthilnathan. N, Sethupathi. P. "Analysis and Prediction of Cogging Torque and Ripples in Output Torque of Permanent Magnet Synchronous Motor and Line Start Permanent Magnet Synchronous Motor". Turkish Journal of Computer and Mathematics Education (TURCOMAT), 2021. 12(3) p. 4586-4595.
[18] D. R. Mandasari, L. Amelia, A. I. Malakaniand, E. D. Purnomo, A. Aziz, A. A. Suryandi, A. Krisnowo, C.S.A. Nandar. Reduction of Cogging Torque in Segmented Permanent Magnet BLDC Motor IPM V-Shape by Skewing Stator. 2022.
[19] S.J. Khare. and R.S. Ambekar. "Comprehensive Design and Study on Cogging Torque Reduction in Permanent Magnet Synchronous Motors for Electric Vehicle Technology". ARAI Journal of Mobility Technology, 2022. 2(3): p. p290-296.
[20] M. Sargazi, M. esmaili, M. Jafarboland, M. khajavi. "Effect of Pole Embrace on The Cogging Torque and Unbalanced Magnetic Forces of BLDC Motors". in 2014 22nd Iranian Conference on Electrical Engineering (ICEE). 2014. IEEE.
[21] Guan R.C, Horng.C. H, and Chun. Y.H, Three-Dimensional Finite-Element Analysis and Optimal Design of Hybrid-Excitation DC Brush Motor for Automotive Engine Start Applications. IEEJ Journal of Industry Applications, 2023. 12(1): p. 65-72.
[22] Jun-Young.K, et al., Effect of Material Characteristics on PMDC Motors based on the Grade of Electrical Steel Sheet. Journal of Magnetics, 2019. 24(2): p. 240-245.